MICROBIOLOGICALLY ACTIVATED CORROSION STUDIES ON DIFFUSION BONDED ALUMINIUM ALLOYS

[1]Venugopal S (Corresponding Author) and [2]Mahendran G
[1]Research Scholar, Department of Mechanical Engineering Sathyabama University,
Chennai-600119, Tamil Nadu, India.
[2]Professor, Department of Mechanical Engineering, IFET College of Engineering,
Vilupuram-605108, Tamil Nadu, India.

Abstract : The aim of this work is to study the effects of corrosion behavior on diffusion bonded AA5083, AA6082 and AA7075 aluminum alloy. The microbiologically influenced corrosion (MIC) behaviour of aluminium alloys is estimated in natural aqueous environment. An optical microscopy is used to confirm the micro colony formation of rod and cocci bacterial species. Polarization study is also carried out to determine the shift in free corrosion potential of metallic structure due to biofilm formation. Corrosion rate is determined by finding the intersection point of E_{corr} and I_{corr} in the polarization curve.AA7075 found to corrode higher than the corresponding welded region of joints. Similarly the corrosion current and corrosion rates are higher for the AA7075 compared to the AA6082 and AA5083. The corrosion rates observed were 2.47, 9.93 and 12.14 mm/year for AA6082, AA5083 and AA7075 respectively at diffusion bonded zones.

Keywords: Diffusion Bonding, Tensile strength, Corrosion rate, Optical microscope, I_{corr}.

I INTRODUCTION

Diffusion bonding provides a novel joining operation for similar (Al-Al alloys)and dissimilar materials (Al-X alloys) without gross microscopic distortion and with minimum dimensional tolerance, the bond strength increased with the increase in bonding temperature and this is essentially due to the increase in the width of the brittle intermetallic compounds[1,2].The bond specific strengths achieved were dependent on interface grain boundary migration and grain growth during the bonding process, and these were considered to be the main mechanisms by which the initial bond interface was removed[3,4].

Strengths are believed to have occurred because of variations in the amount of liquid gallium[5]. Bonding temperature due to the formation of finer size intermetallic compounds and good bonding between mating surfaces, Increases in the joining temperature cause the volume fraction of intermetallics to increase. These intermetallics lower the strength of diffusion bonds when proposed at higher temperature[6]. Bonding time increases the hardness of the joint interface increases due to intermetallic compounds formation, with the increasing of bonding time, the shear strength of the joints increases due to diffusion of atoms in the interface [7].Hence, the diffusion bonding technique to join these dissimilar materials[8].. The selection of diffusion bonding process variables affecting the interface structure, compound formation and morphology is critical to attain good quality bonds. The predominant process parameters in diffusion bonding process are: (bonding) temperature (bonding) pressure and (holding) time [9].

However, the bonded aluminium alloys shows more susceptible to corrosion by attack from halide ions such as chlorides. This susceptibility to localized corrosion appears to make aluminium alloys vulnerable to MIC. Contaminants in the fuel such as surfactants, water and water-soluble salts may contribute to bacterial growth. The two mechanisms for MIC of aluminium alloys have been documented: the production of water-soluble acids by bacteria and fungi, and the formation of differential aeration cells [10].

Microbial colonization of metal surfaces causes severe change in the ions concentration, pH, conductivity, and redox potential, altering the passive or active behaviour of the metallic substratum and its corrosion products, as well as the electrochemical variables. Micro organisms influence corrosion by changing the electrochemical conditions at the metal–solution interface. These changes may have different effects, ranging from the induction of localized corrosion to corrosion inhibition through a change in the rate of general corrosion, [11].

A proper identity of bacteria by which corrosion may be exploited on metal surface and role of microbial contaminants in the specific environment as a useful tool to prevent frequent MIC effects [12]..

Very few investigations evaluated the diffusion bonding of aluminium materials. Moreover, those literatures are focusing on

microstructure analysis, phase formation studies, hardness survey at the interface and their subsequent influence on bonding strength. Hence, the present investigation was carried and assessed to elucidate microbial corrosion behaviour of aluminium alloys in natural aqueous environment. Biomass is evaluated as a spectrophotometric analysis of carbohydrate and protein content. The bacterial colonies are expressed as colony-forming units per ml (CFU/ml). The bacterial species are identified up to genus level by employing morphological and biochemical characterization.

II. EXPERIMENTAL WORK

2.1 Fabricating the joints and preparing the specimens

Rolled plates of 5 mm thick AA5083 aluminium alloys are used in this investigation. The chemical composition and mechanical properties of the AA5083 are presented in Tables 1 & 2. The plate was cut to the required size (50 x 50 mm) by power hacksaw followed by milling. The bonding surfaces of samples were ground flat by 200, 400 and 600 grit SiC papers and cleaned in acetone prior to diffusion bonding. The polished and chemically treated specimens were covered at the bottom and top with a mica sheet (RUBY) in a die made up of H-13Tool Steel, and were inserted into a vacuum chamber (vacuum pressure of 29Hg was maintained).

Table 1 Chemical Composition (wt. %) aluminium alloy

Sample	Si	Fe	Cu	Mn	Mg	Cr	Zn	Ti	Others	Al
AA5083	0.26	0.35	0.05	0.60	4.74	0.11	0.05	0.06	0.01	
AA6082	1.1	0.5	0.1	0.4	1.0	0.25	0.2	0.1	0.15	Balance
AA7075	0.4	0.5	1.2	0.3	2.1	0.21	5.6	0.2	0.05	

The specimen is heated up to the bonding temperature by using the induction furnace with a heating range of 25ºC/min. simultaneously; the required bonding pressure was applied with the holding time. After the completion of bonding, the samples are cooled to room temperature before taking away from the chamber.

Table 2 Physical and Mechanical Properties of aluminium alloy

Sample	Density (g/cm^3)	Melting Point (ºC)	Ultimate Tensile Strength (MPa)	Yield Strength (MPa)	Elongation (%)	Poisson's Ratio	Crystal Structure
AA5083	2.7	665	290	145	22	0.3	
AA6082	2.7	665	305	271	12	0.3	FCC
AA7075	2.80	635	572	331	11	0.33	

2.2 Recording the responses

After the bonding process, the samples were prepared from the Al/Al diffusion bonded joints using a wire-cut EDM, the tensile test was carried out in 50 KN capacity servo controlled universal testing machine. Determine the mechanical properties of the bonding and shear-tensile test were carried out on the diffusion bonded samples, to measure shear strength of the joints, lap joint samples were prepared in accordance with ASTM Standard D1002-99. The diffusion bonded side was etched with a Keller's solution (3ml HCl, 2 ml HF and 90 ml distilled water). The test specimens were polished in disc polishing machine for scratch fewer surfaces and the surface.

Biofilms are consented to grow on metal surfaces using 1% of glucose as nutrient to natural lake water under laboratory conditions. The contamination of water is avoided by adding 25 ml of fresh natural lake water after the same quantity of water is pipetted out from the system for every five days. The chemical constituents of water sample, such as, water temperature, pH,

conductivity and dissolved oxygen concentration are measured throughout the experiment. All the experiments are carried out at constant atmospheric conditions.

An UV-VIS spectrophotometer is used for carbohydrate and protein content analysis (M/s Shimadzu, Japan). Micro colony confirmation is done by an optical microscopy with CCD camera (M/s Shimadzu, Japan). Enumeration of viable cell can be counted by plate count technique using digital colony counter (M/s ELICO, India). The polarization studies are carried out using Potentiostat/Galvanostat (M/s Princeton, Model No. 362). All the chemicals used in this experiment, are purchased from M/s Fluka.

2.3 Biomass measurement

Biofilm samples for mass analysis are obtained from the outer surface of each metal at the end of experiments. Biomass data represents the average of ten measurements from the same sample. The biofilm samples from the respective metal are subjected for the analysis of carbohydrates and protein. The analysis of carbohydrates involves the treatment of samples with sulphuric acid to cause the hydrolysis of glycosidic linkages and to dehydrate the monosaccharide in order to allow the reaction with anthrone to yield blue-green coloured complex which is measured calorimetrically at 660 nm, [13]. Bradford protein assay is based on the observation that the absorbance maximum for an acidic solution of Coomassie Brilliant Blue G-250 shifts from 465 nm to 595 nm when binding to protein occurs observed [14]. The metal biofilm samples are also subjected to determine the presence of sulphate reducing bacteria. The detection of sulphate reducing bacteria in biofilm samples can be performed using the method developed by the American Petroleum Institute.

2.4 Identification of bacteria

The biofilm samples are carefully scraped with a non-metallic spatula and are serially diluted. Then the samples are plated on nutrient agar medium to enumerate the heterotrophic bacteria, [15].The bacterial colonies are expressed as colony-forming units per ml (CFU/ml). The most numerous similar colonies from all plates are identified through their morphological and biochemical characteristics, [16].

2.5 Electrochemical study

The biofilm growth on metal surface can influence a change in free corrosion potential and also corrosion current. Corrosion potential and corrosion current of biofilm adhered aluminium alloy is measured against a saturated calomel reference electrode (SCE). The working electrodes constitute test material of 1 cm^2 of test area. All the experiments are carried out at constant temperature with natural lake water as an electrolyte. The slope of the polarization curve can be used to characterize the degree to which any stage of anodic or cathodic processes is inhibited. The coordinates of this point define the free corrosion potential of the system, as well as total corrosion current ($I_{corr}=I_{anodic}=I_{cathodic}$). The intersecting point of E_{corr} and I_{corr} in the polarization curve can be used to determine the corrosion rates through the Faradays law equation (1) [16].

$$\text{Corrosion Rate (CR)} = (I_{corr} * M)/zAF\rho \quad (1)$$

where CR is the corrosion rate (mm/yr), I_{corr} is the corrosion current (A), M is the molar mass of metal (g/mole), A is area of electrode (mm^2), z is number of electrons transferred per metal atom, F is the Faraday's constant and ρ is the density of metal (g/mm^3).

III. RESULTS AND DISCUSSION

3.1 Bacteria identification

The biofilm structures of all the three metal samples are confirmed on examination under a computer enhanced optical microscopy with CCD camera. The CCD image of dominant bacterial species *Pseudomonas* in diffusion bonded AA7075 alloy is shown in Fig. 1.

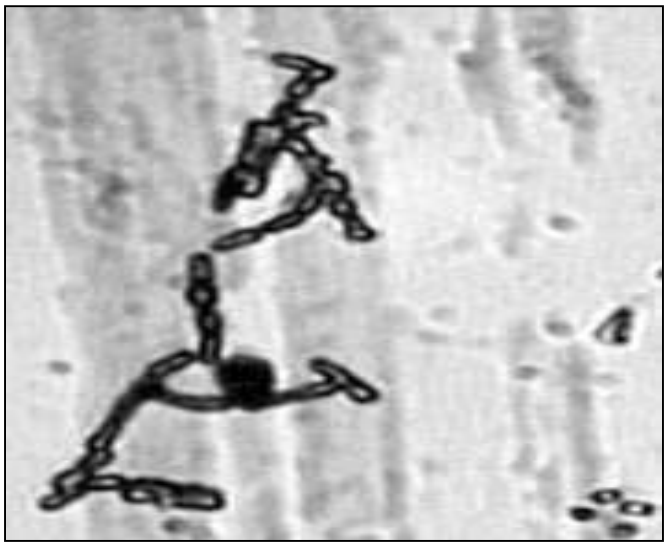

Fig. 1 CCD image of dominant bacterial species *Pseudomonas*

A mixture of micro colony formation, including rod shaped bacteria and cocci are identified through microscopic analysis. The viable cell counts after one month are averaged $1810x10^7$ CFU/ml in diffusion bonded AA7075 aluminium alloy. The biofilm sample is subjected to find out the presence of sulphate reducing bacteria. Based on the results of sulphate reducing bacteria determination, it is confirmed that the biofilm sample is not constituted with sulphate reducing bacteria. The changes in chemical constituents of water, such as pH, conductivity and dissolved oxygen after one month are averaged given in the Table 3.

Table 3 Analysis of Chemical Constituents of Water

Samples	Biomass (mg/ml)		Cell Count (CFU/ml)	Dominant Species	E_{corr} (mV) vs. Ag/AgCl)	I_{corr} (mA/cm^2) x 10^{-3}	Corrosion Rate (mm/year)
	Carbohydrate	Protein					
AA7075	0.3935	0.1914	$1810x10^7$		-890	0.9116132	9.9274
AA6082	0.3145	0.1841	$1722x10^7$	*Pseudomonas*	-740	0.2272643	2.4749
AA5083	0.2897	0.1624	$1628x10^7$		-690	1.115	12.142

3.2 Corrosion test analysis sample for corrosion studies

Table 3 shows the corrosion rate of aluminium alloys. It is observed that AA7075 aluminium alloy shows higher rate of corrosion. Polarization resistance measurements are an accurate and rapid way to measure the general corrosion rate. Electrochemical polarization test methods are extremely pertinent for understanding and evaluating the corrosion behavior of materials with changes in the exposed corrosive environment. The results of potentiodynamic corrosion studies would throw light on suitability of alloys for anodic or cathodic protection and susceptibility to several forms of corrosion. It is observed that corrosion resistance of weld metal is better than that of TMAZ (Thermo mechanical affected zone) and base metal.

In AA7075 is susceptible to galvanic attack near precipitates of $MgZn_2$ MgAlCu. The general corrosion resistance of the AA6082 parent material is better than the AA7075 parent material due to content of copper. The zinc rich precipitates in the AA7075 alloy causes the formation of micro galvanic cells, leading to higher rates of dissolution. Further, zinc is active when compared to aluminum alloy matrix, hence can enhance the corrosion rate. The potentiodynamic polarization curves for alloys under study are shown in Fig 2.

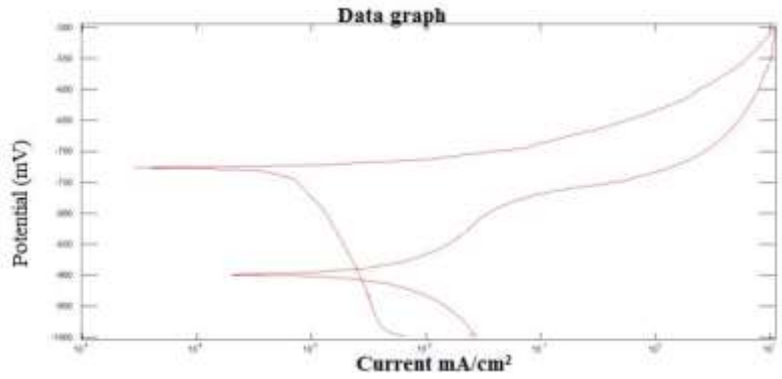

(a) AA5083

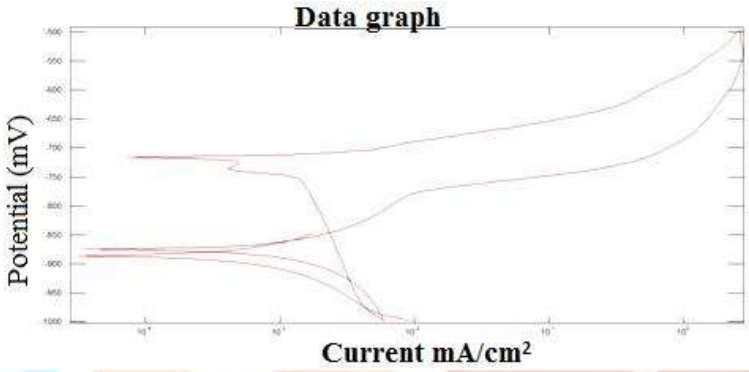

(b) AA6082

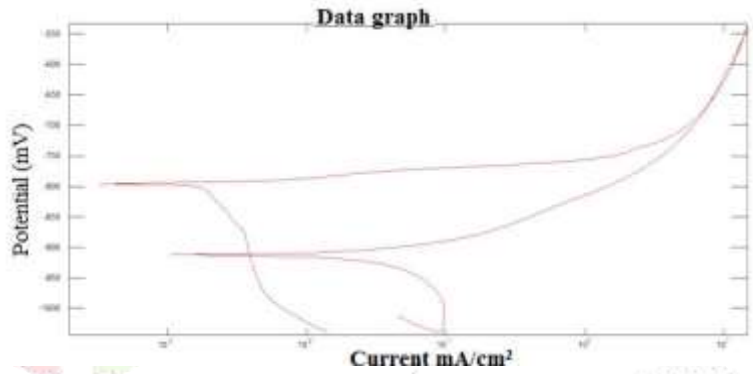

(c) AA7075

Fig. 2 Polarization curve of diffusion bonded Aluminium alloys

It is observed that the diffusion bonded AA7075 shows higher corrosion rate of 12.142 mm/year followed by AA5083 parent metal imparts 9.9274 mm/year while AA6082 parent metal imparts 2.4749 mm/year with better corrosion resistant properties. This result indicate that the sample AA6082 of the diffusion bond joint act as a cathode and give better resistance to corrosion when compared to samples AA7075& AA5083.

3.3 Effect of Microstructure on Corrosion rate

The microstructure of the diffusion bonded zones of AA5083, AA6082 and AA7075 aluminium alloy are shown in Fig. 3.

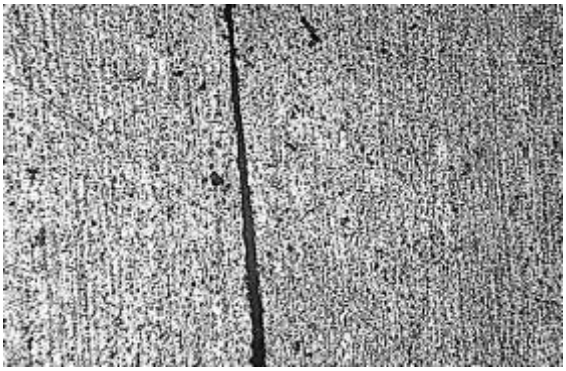

(a) AA5083

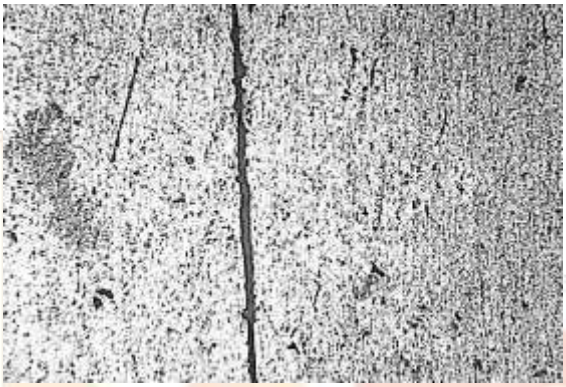

(b) AA6082

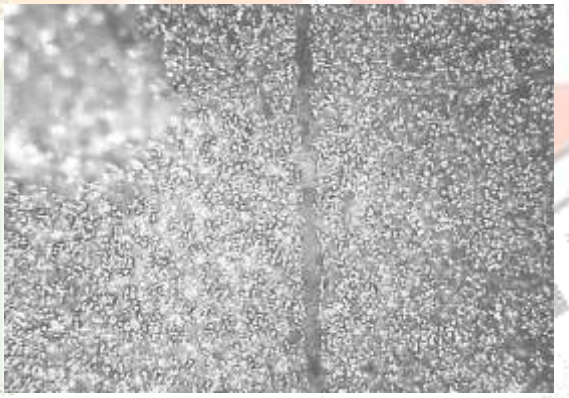

(c) AA7075

Fig. 3 Microstructure of diffusion bonded Aluminium alloys after corrosion test

The effect of polarization leads to the formation of large corrosion pits. These pits are shown in black color cylindrical shape and occurred in close proximity. In addition the grains boundaries are ditched and nowhere the surface of the metal is free from corrosion pits. Fig 2 shows the micro structure of alloys after potential-dynamic polarization. As stated above the corrosion pits are in the same order of corrosion rate. The effect of polarization leads to the formation of corrosion pits of different gravity. The three corrosion surface images are taken from the fusion zone. The affected zone of the weld exhibited highest susceptibility to inter-granular corrosion[17,18]. This zone does not show the presence of deep pits instead, the grain boundaries are marginally ditched. The constituents of the fusion zone are more diluted with AA7075alloy. Hence the corrosion behavior is more and follows the pattern of AA7075. However the corrosion rate is the consolidated effect of the entire three zones as the corrosion cell covers all the three zones. In AA7075, parameter the effect of polarization leads to the formation of corrosion pits of different gravity[19].The three corrosion surface images are taken from the fusion zone. Severe corrosion pits as well as grain boundary ditches but there are more resistance to corrosion while compare to other zones. It is evident that this surface should have shown more corrosion and the experimental values confirm the same[20].

IV. CONCLUSION

i. The present work investigated the corrosion behavior of diffusion bonded AA5083, AA6082, AA7075 aluminum alloys. The findings made by the experimental work are given below.

ii. Out of the diffusion bonded alloys, AA6082 showed low corrosion rate of 2.47 mm per year. AA5083 diffusion bonded zone showed 9.92 mm per year followed by AA7075 with high corrosion rate of 12.142mm per year with least corrosion resistance.

iii. The rest potential vary in the order AA7075 > AA5083 > AA6082. Comparison of microstructure before and after potentiodynamic polarization corrosion pits in the order AA7075 > AA5083 > AA6082.

iv. The corrosion rate of the three diffusion bonded similar alloys are in the order AA7075 > AA5083 > AA6082

REFERENCES

[1]. Kundu S and Chatterjee S. Interfacial Microstructure and Mechanical Properties of the Diffusion Bonded Joints of Titanium to Stainless Steel with Nickel Interlayer. Mater Sci Eng A 425 (2006)107-113

[2]. Ghosh M, Bhanumurthy K, Kale G B, Krishnan J and Chatterjee S. Diffusion bonding of titanium to 304 stainless steel. Journal of Nuclear Materials 322 (2003) 235-241.

[3]. Kundu S, Ghosh M, Laik A, Bhanumurthy K, Kale G B and Chatterjee S. Diffusion bonding between commercially pure titanium and 304 stainless steel using copper interlayer. Materials Science and Engineering A 407(2005)154-160

[4]. Huang Y, Ridley N and Humphreys F J. Diffusion bonding of superplastic 7075aluminium alloy. Materials science and Engineering A 266(1999) 295-302.

[5]. Shirzadi A A, Saindrenan G and Wallach E R. Diffusion Brazing of Aluminium-Based Materials Using Gallium. Materials science Forum 396-402 (2002) 1579-1584.

[6]. Ghosh M and Chatterjee S. Diffusion bonded transition joints of titanium to stainless steel with improved properties. Materials Science and Engineering A 358 (2003)152-158.

[7]. Kenevisi M S and Mousavi Khoie S M. A study on the effect of bonding time on the properties of AL7075TOTi-6AL-4V diffusion bonded joint. Materials letters 76 (2012)144-146.

[8]. Yeh M S and Chuang T S. Low Pressure Diffusion Bonding of SAE 316 Stainless Steel by Inserting a Super Plastic Interlayer. Scripta Metallurgica Materialia, 33 (1995),1277-1281.

[9]. Feng J C, Zhang B G, Qian Y Y and He P. Microstructure and Strength of Diffusion Bonded Joints of Ti Al Base Alloy to Steel Material Characterization 48 (2002) 401-406.

[10]. Little B, Wagner P, Mansfeld, F. Microbiologically influenced corrosion of metals and alloys, International Materials Review 36(6), (1991) 253-257

[11]. Beech IB, Sunner JA. Biocorrosion: towards understanding interactions between biofilms and metals,.Curr. Opin. Biotechnol 15(3),(2004), 181-186

[12]. Videla HA, Herrera LK, Microbiologically influenced corrosion: looking to the future, International microbiology 8, (2005),169-180

[13]. Sadasivam S, Manickam A, Biochemical methods for Agricultural sciences, Wiley Eastern Limited, New Delhi, 1992

[14]. Bradford MM. A rapid and sensitive for the quantization of microgram quantities of protein utilizing the principle of protein-dye binding, Analytical Biochemistry 72, (1976), 248-254

[15]. Staley JT, Bryant MP, Pfenning N, Bergey's Manual of Systematic Bacteriology, Vol 3, Williams & Wilkins, 1989.

[16]. Murugesan AG, Rajakumari C. Environmental Science and Biotechnology, Vol 1, MJP publishers, 1995

[17]. Abbasi M, Karimi Taheri A and Salehi M T. Growth rate of intermetallic compounds in Al/Cu bimetal produced by cold roll welding process. J Alloy Compd 319 (2001) 233-241.

[18]. He P and Liu D. Mechanism of forming interfacial intermetallic compounds at interface for solid state diffusion bonding of dissimilar materials. Mater Sci Eng A 437 (2006) 430-435.

[19]. Smith W F, Principles of Materials Science and Engineering, McGraw-Hill publishing Company, 2nd edition, New York (1990).

[20]. Wert J A, Paton N E, Hamilton C H, and Mahoney M W. Grain refinement in AA 7075 aluminum by thermo-mechanical processing. Metall. Trans. 12A (1981) 1267.